AD-A132 493 SURVEILLANCE PROTOTYPE INTERIOR ENTRY (SPIE) PROJECT (U) SCIENCE APPLICATIONS INC TUCSON AZ D G CROWE 25 JUL 83 DAAK70-82-C-0120 1/1

UNCLASSIFIED F/G 15/4 NL

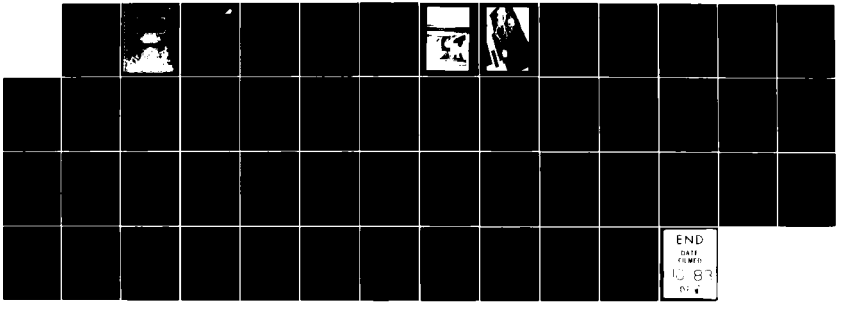

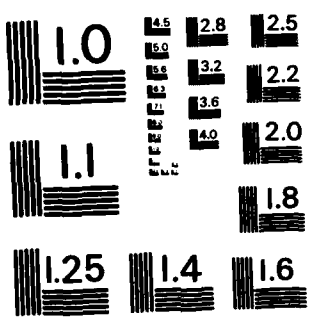

SPIE PROJECT

FINAL REPORT

Contract DAAK-70-82-C-0120

SUBMITTED TO:

NIGHT VISION AND ELECTRO-OPTICS LABORATORY
ATTN: WILLIAM JOHNSON
SPO-SID-DELNV-SD
MERADCOM
FT. BELVOIR, VA 22060

PREPARED BY:

DEVON G. CROWE
SCIENCE APPLICATIONS, INC.
5151 E. BROADWAY, SUITE 1100
TUCSON, AZ 85711

JULY 25, 1983

TABLE OF CONTENTS

1.0 INTRODUCTION

The U.S. Army has the potential need to perform real-time surveillance of interior spaces during hostage events. SAI has delivered a Surveillance Prototype, Interior Entry (SPIE) device to the Army. The delivery of this device constituted fulfillment of the original contract. Consultation between SAI and the Army identified additional tasks which were also provided, as described in Section 2.

2.0 SPIE DEVICE AND USER AGENCY SUPPORT

An SPIE device was delivered to the Army under contract number DAAK70-82-C-0120 on August 11, 1982. Figures 1 and 2 illustrate the principal components. Figure 1 shows a low light level television (L^3TV) camera coupled to a cystoscope and mounted on a tripod. The cystoscope has an outside diameter of 0.19 inches which allows it to be inserted through a hole in the wall, a keyhole, or, in some cases, under a door. The cystoscope has 45 optical elements and provides a high quality image; however, there is sufficient light loss that an L^3TV is required to provide a high signal-to-noise ratio under realistic ambient light levels. The wide field of view (about 80°) and the 30° angle between the optical axis and the axis of the physical cylinder which houses the lenses allows essentially an entire room to be examined with a single penetration into the space. Rotation of the cystoscope brings different portions of the room into the field of view.

Figure 2 shows an alternate configuration in which the cystoscope is coupled to a fiber optic bundle and eyepiece to allow direct viewing with the human eye. The principal limitations to the performance in this configuration are the additional light loss in the fiber optic and the limited resolution of about 290 lines per picture height due to the finite number of optical fibers in the bundle (about 65,000).

Additional user agency support in the areas of portable night-lights, sound masking and cancellation, and the identification of follow-on efforts was provided as summarized in Table 2.1. The Army user agency

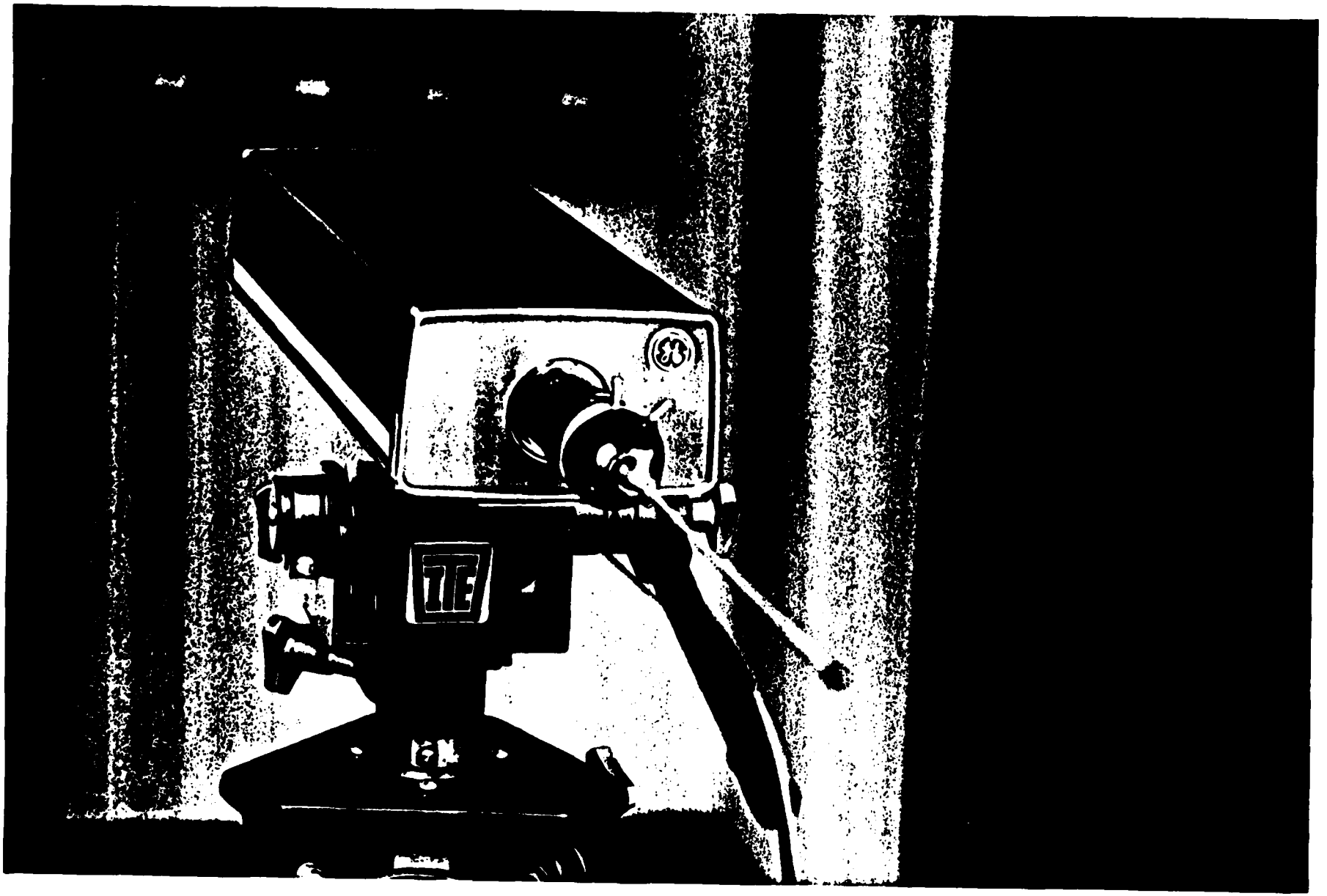

FIGURE 1. SPIE LOW LIGHT-LEVEL CAMERA WITH CYSTOSCOPE

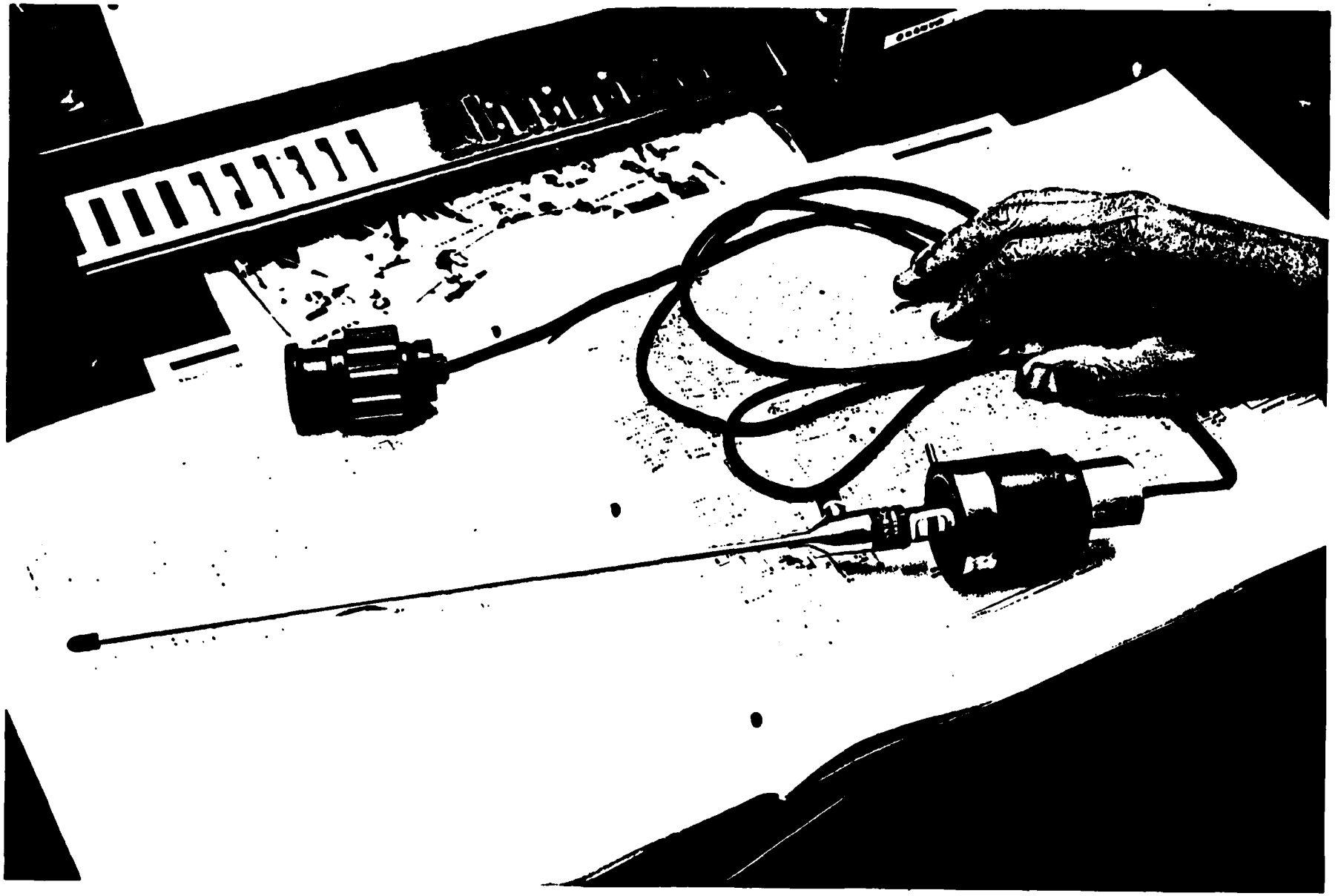

FIGURE 2. CYSTOSCOPE COUPLED TO FIBER OPTIC BUNDLE WITH EYEPIECE

was also supported in briefing Pentagon officials. The unique and varied requirements of the Army user agency for technical assistance could only be met through a flexible approach to setting priorities in consultation with the Army. It is anticipated that follow-on efforts will also be characterized by a dynamic and flexible response to the needs of the army.

Technical analyses necessary to the performance of the tasks in Table 2.1 are provided in Appendices A through E.

TABLE 2.1

SPIE PROJECT TASKS

1. PRELIMINARY ELECTRO-OPTICAL DEVICE PERFORMANCE CALCULATIONS
   -- Estimated Possible Device Performance
2. ELECTRO-OPTICAL DEVICE ASSEMBLED, DELIVERED, AND CUSTOMER EVALUATED
   - System Components:
     -- Low Light Level Television (L^3TV) Camera
     -- Two Cystoscope Optical Assemblies
     -- Flexible Fiber Optic Imaging Link
     -- Optical Coupling Assemblies
     -- Television Monitor
     -- Tripod
     -- Cables
     -- Manuals
   - Delivered August 11, 1982
3. HIGH INTENSITY PORTABLE NIGHT LIGHT EXPERIMENTAL PROTOTYPES DELIVERED FOR EVALUATION
4. SOUND MASKING EQUIPMENT DELIVERED AND TESTED
   - System Components:
     -- Tape Player
     -- Speakers
     -- Custom Sound Effects Tapes
5. SILENT DRILLING CONCEPT FORMULATED
6. PRELIMINARY SOUND CANCELLATION EXPERIMENTS PERFORMED
   -- Limited Cancellation ($\sim$ 6 dB) Achieved
7. SOUND CANCELLATION SENSITIVITY CALCULATION DOCUMENTED
8. UHF TELEVISION JAMMING EXAMINED

(Cont'd)

TABLE 2.1 (Cont'd)

9. IDENTIFICATION OF POSSIBLE FOLLOW-ON EFFORTS:

- Prototype Improved Multiple Integrated Laser Engagement System (MILES)
- Cystoscope/Microchannel Plate (MCP/Flexible Fiber Optic/ Eyepiece Combination

  -- Provides Self-Contained Portable System
- Custom High Resolution (400,000 Fibers) Flexible Fiber Optic
- Power Zoom Optics For L^3TV Camera
- Custom Repackaged Cystoscope With 30° Bend And Small Diameter
- MCP Intensified CCD L^3TV Camera For Compactness And Light Weight
- Technical Consulting Support As Required

10. PENTAGON ARMY OFFICIALS BRIEFED ON THE IMPORTANCE OF THE EFFORT BY REPRESENTATIVES OF SAI AND THE ARMY USER AGENCY

3.0 SUMMARY

A prototype SPIE device was delivered in a timely fashion in fulfillment of the contracted effort. Additional Army user agency support in a number of other areas was provided, as described in Section 2.0 and the Appendices.

The needs of the Army user agency are still evolving and are not yet fully defined. SAI is prepared to continue the type of flexible support demonstrated under the present contract in future follow-on efforts.

The SPIE device which has been delivered fully meets its design requirements and performs satisfactorily. The lightweight, portable, second-generation equipment proposed for the follow-on effort is anticipated to be capable of superior low-light level performance as well as compactness.

APPENDIX A

PRELIMINARY PERFORMANCE ANALYSIS OF LOW-LIGHT LEVEL TELEVISION/ CYSTOSCOPE COMBINATION

Summary

It is found, using several assumptions which are detailed in this memo, that the SPIE device should be capable of imaging room scenes from high lighting levels appropriate for reading and close work, down to objects of 50% reflectivity illuminated only by a television screen 10 feet away from the objects.

Protection from bright light damage and mechanical ruggedness should be given careful attention in TV camera selection.

BRIGHTNESS OF ROOM OBJECTS

The range of brightness (luminance) for objects in a room under a variety of illumination conditions of interest is shown to vary from approximately 3×10^{-3} foot Lamberts (fL) to 30 fL. Photometric units (based upon the lumen which involves the spectral response of the eye) are used instead of radiometric units (based upon the watt), because most low light level TV camera specifications are made in this system. It is assumed for convenience that all objects are Lambertian reflectors. This is essentially true for many objects, the exceptions being exceptionally smooth surfaces, such as plate glass and polished metal. Smooth surfaces reflect almost entirely in the specular direction and the brightness of the same object will vary with orientation. The brightness

of smooth, highly reflective objects can vary from essentially zero to the brightness of the room lighting. The maximum brightness of artificial room lighting will be approximately 100 foot candles (fc).

The upper end of the range of room object brightnesses is determined by a white (reflectance, $\rho = 1$) object adjacent to the maximum assumed ambient lighting of 100 fc. This object brightness is $100/\pi \approx 30$ fL.

The lower end of the range of room object brightnesses will now be estimated. The number of lumens incident on an object (Φ) due to a source of brightness L_s(fL) at a distance R (feet) is:

$$\Phi = \frac{L_s A_s \cos\theta_s A_o \cos\theta_o}{R^2} \qquad (1)$$

where A_s is the area of the source (ft^2), A_o is the area of the object, θ_s is the angle of the (flat) source with the direction of propagation to the object, and θ_o is the angle the (flat) object surface makes with that direction. The resulting brightness for a Lambertian object (reflecting into π steradians) of reflectance ρ is:

$$L_o = \frac{\rho \Phi_o}{\pi A_o} \qquad (2)$$

Substituting Eq. (1) for Φ_o into Eq. (2):

$$L_o = \frac{\rho L_s A_s}{\pi R^2} \quad , \qquad (3)$$

if $\cos\theta_s = \cos\theta_o = 1$.

The object of minimum brightness is assumed to have $\rho = 0.1$ and is illuminated by a 17" diagonal television screen ($A_s \approx 1\ ft^2$) at a distance of 10 feet. The television screen brightness is assumed to be 10 fL. We have then:

$$L_{o_{min}} = \frac{0.1(10)(1)}{\pi(10)^2} \approx 3 \times 10^{-3}\ fL \quad .$$

RADIATIVE TRANSFER

A convenient form for the luminous flux incident on an optical receiver due to a bright object is:

$$\Phi_r = \tau L_o A_r \Omega_r \quad , \tag{4}$$

where A_r is the aperture area of the receiver, τ is the transmittance, and Ω_r is the solid angle field of view of the receiver. Equation (4) assumes that the entire field of view is filled with a scene of average brightness L_o.

If the received luminous flux is optically coupled to another optical instrument (e.g., a cystoscope is coupled to a T.V. camera), then the illuminance (fc) incident on the second instrument is:

$$E_i = \frac{\Phi_r}{A_i} = \tau L_o \Omega_r \left(\frac{A_r}{A_i}\right) \quad , \tag{5}$$

where A_i is the aperture area of the second instrument. Equation (5) assumes that all of the light is coupled to A_i.

CYSTOSCOPE PARAMETERS

It is assumed that the cystoscope consists of 15 triplet relay lenses arranged in a tube which is absolutely black on the inside. If this tube is partially reflective on the inside, ghost images will appear in the output which degrade performance, but which do not contribute to the brightness of the primary image. It is further assumed that the lenses are free of aberrations. Aberrations would reduce the brightness of the primary image.

The reflectance of a single triplet relay lens is derived in Appendix A.1. This derivation allows three different indices of refraction for the three lens elements, and off-axis angles of incidence are treated. For this preliminary analysis, the on-axis reflectance only will be calculated. The normal incidence reflectances at each interface are:

$$\rho_i = \left[\frac{n_{i-1} - n_i}{n_{i-1} + n_i}\right]^2_{i=1,2,3,4} , \tag{6}$$

where n_0 and n_4 are the index of refraction of air and n_1, n_2, n_3 are the indices of the three lens elements. The overall reflectance from Appendix A for the triplet, taking into account the infinite series of reflections of reflections is:

$$\rho = \rho_1 + \frac{\rho_2(1-\rho_1)^2}{1-\rho_1\rho_2} + \frac{\rho_3(1-\rho_1)^2(1-\rho_2)^2}{1-\rho_2\rho_3} + \frac{\rho_4(1-\rho_1)^2(1-\rho_2)^2(1-\rho_3)^2}{1-\rho_3\rho_4} \tag{7}$$

It is assumed that $n_1 = 1.5$, $n_2 = 1.7$, and $n_3 = 1.6$, then

$$\rho_1 = 0.04, \quad \rho_2 = 0.0039, \quad \rho_3 = 0.00092, \quad \rho_4 = 0.053 \ .$$

The overall reflectance of the triplet from Eq. (7) is:

$$\rho = 0.0928 \ .$$

The overall transmission for 15 triplets in series with no other reflections is then:

$$\tau_{total} = (1 - \rho)^{15} = (0.9072)^{15} = 0.232 \ .$$

The solid angle field of view of the cystoscope is estimated from the statement by Peter Franken that there is about a 100° field of view. This corresponds to a cone subtending about 2.8 steradians.

It is assumed that the cystoscope has a clear aperture of 1.5 mm diameter.

DISCUSSION

Equation (5) can be used with the assumed cystoscope parameters to discuss the projected performance of a low-light level television (LLLTV) coupled to the cystoscope. If the LLLTV has an aperture of 30 mm, then:

$$E_i = 0.232 \ L_o (2.8) \left[\frac{\frac{\pi}{4}(1.5)^2}{\frac{\pi}{4}(30)^2} \right] = 1.6 \times 10^{-3} \ L_o \ , \qquad (8)$$

where, it will be remembered, the E_i is the incident illuminance on the LLLTV in foot candles, and L_o is the room luminance in foot Lamberts. The range of room luminance is 3×10^{-3} fL to 30 fL. From Eq. (8) then:

$$4.8 \times 10^{-6} \text{ fc} \leq E_i \leq 4.8 \times 10^{-2} \text{ fc} \quad . \tag{9}$$

This may be compared with the "minimum required illumination" for the Panasonic W-1910 Stellar Lite Camera of 2.5×10^{-5} fc. At a distance of 10 feet from a television screen illumination source, an object with $\rho > 0.5$ would be detectable under the assumptions of this preliminary calculation.

It should be mentioned that in addition to sensitivity, major considerations in camera selection include protection from bright sources, and mechanical ruggedness. I suggest that a second or third generation LLLTV using micro-channel plate technology be selected. This offers the advantages of electronic limiting (Figure 1) which is much faster than a mechanical iris alone, and a low operating voltage (2-5 KV, instead of 20-50 KV).

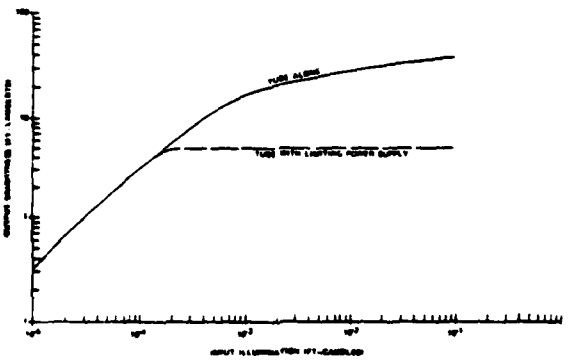

Figure 8.
THE TYPICAL INTENSIFIER GAIN SATURATION CHARACTERISTICS OF AN MCP INTENSIFIER TUBE AS COMPARED TO AN MCP INTENSIFIER TUBE THAT HAS AUTOMATIC POWER SUPPLY CIRCUITS TO PREVENT DAMAGE TO THE TUBE AT RELATIVELY HIGH LEVELS OF ILLUMINATION WHILE MAINTAINING A CONSTANT SCREEN BRIGHTNESS.

APPENDIX A.1.
REFLECTANCE OF A THREE-LAYER DIELECTRIC

A single-layer dielectric coating will first be modeled so that the reader may more easily visualize how a three-layer model is constructed.

In Figure A1, an irradiance E (watts per square centimeter) is incident at the upper left. The refractive index of the immersion medium (air) is n_0; the index of the transparent (no absorption) dielectric coating is n_1; and the index of the substrate is n_2. The substrate is assumed to have no internal transmittance, while the dielectric is assumed to have no internal absorption. The reflectance at the first surface for the case of normal incidence is:

$$\rho_1 = \left[\frac{n_0 - n_1}{n_0 + n_1}\right]^2 \quad . \tag{A-1}$$

Similarly,

$$\rho_2 = \left[\frac{n_1 - n_2}{n_1 + n_2}\right]^2 \tag{A-2}$$

at normal incidence. The reflectances for other than normal incidence with unpolarized irradiance are:

$$\rho_1 = \frac{1}{2}(\rho_n + \rho_p) = \frac{1}{2}(r_n^2 + r_p^2)$$

$$= \frac{1}{2}\left[\frac{\sin^2(\theta_i - \theta_t)}{\sin^2(\theta_i + \theta_t)} + \frac{\tan^2(\theta_i - \theta_t)}{\tan^2(\theta_i + \theta_t)}\right] \quad , \tag{A-3}$$

and

$$\rho_2 = \frac{1}{2}\left[\frac{\sin^2(\theta_i' - \theta_t')}{\sin^2(\theta_i' + \theta_t')} + \frac{\tan^2(\theta_i' - \theta_t')}{\tan^2(\theta_i' + \theta_t')}\right] \quad , \tag{A-4}$$

where ρ_n is the power reflectance for light polarized normal to the incident plane (the plane in which Figure A1 lies); ρ_p is the power reflectance for light polarized parallel to the incident plane; r_n is the amplitude reflectivity for light polarized normal to the plane; r_p is the amplitude reflectivity for light polarized parallel to the plane; and

$$\theta_i \pm \theta_t = \theta_i \pm \arcsin\left[\frac{n_o}{n_1} \sin \theta_i\right] \quad , \tag{A-5}$$

and

$$\theta_i' \pm \theta_t' = \theta_t \pm \theta_t' = \arcsin\left[\frac{n_o}{n_1} \sin \theta_i\right] \pm \arcsin\left\{\frac{n_1}{n_2}\left(\frac{n_o}{n_1} \sin \theta_i\right)\right\} \quad , \tag{A-6}$$

where θ_i is the initial incident angle, as illustrated in Figure A1.

The total power reflectance is the sum of all of the individual reflectances (the first three are illustrated in Figure A1):

$$\rho = \rho_1 + (1 - \rho_1)^2 \sum_{n=0}^{\infty} \rho_1^n \rho_2^{n+1} \quad , \tag{A-7}$$

where it should be remembered that there is no absorption in the dielectric and complete absorption in the substrate. Equation (A-7) can be summed exactly after rewriting it as a geometric series:

$$\rho = \rho_1 + \rho_2(1 - \rho_1)^2 \sum_{n=0}^{\infty} (\rho_1 \rho_2)^n$$

$$= \rho_1 + \frac{\rho_2(1 - \rho_1)^2}{1 - \rho_1 \rho_2} \quad . \tag{A-8}$$

The geometric series corresponding to Eq. (A-8) for the three dielectric case is:

$$\rho = \rho_1 + \rho_2(1-\rho_1)^2 \sum_{n=0}^{\infty} (\rho_1\rho_2)^n$$

$$+ \rho_3(1-\rho_1)^2(1-\rho_2)^2 \sum_{n=0}^{\infty} (\rho_2\rho_3)^n$$

$$+ \rho_4(1-\rho_1)^2(1-\rho_2)^2(1-\rho_3)^2 \sum_{n=0}^{\infty} (\rho_3\rho_4)^n \quad . \qquad \text{(A-9)}$$

This may be summed exactly:

$$\rho = \rho_1 + \frac{\rho_2(1-\rho_1)^2}{1-\rho_1\rho_2} + \frac{\rho_3(1-\rho_1)^2(1-\rho_2)^2}{1-\rho_2\rho_3}$$

$$+ \frac{\rho_4(1-\rho_1)^2(1-\rho_2)^2(1-\rho_3)^2}{1-\rho_3\rho_4} \qquad \text{(A-10)}$$

These equations assume that the dielectric (glass) itself is "lossless" and not anti-reflection coated.

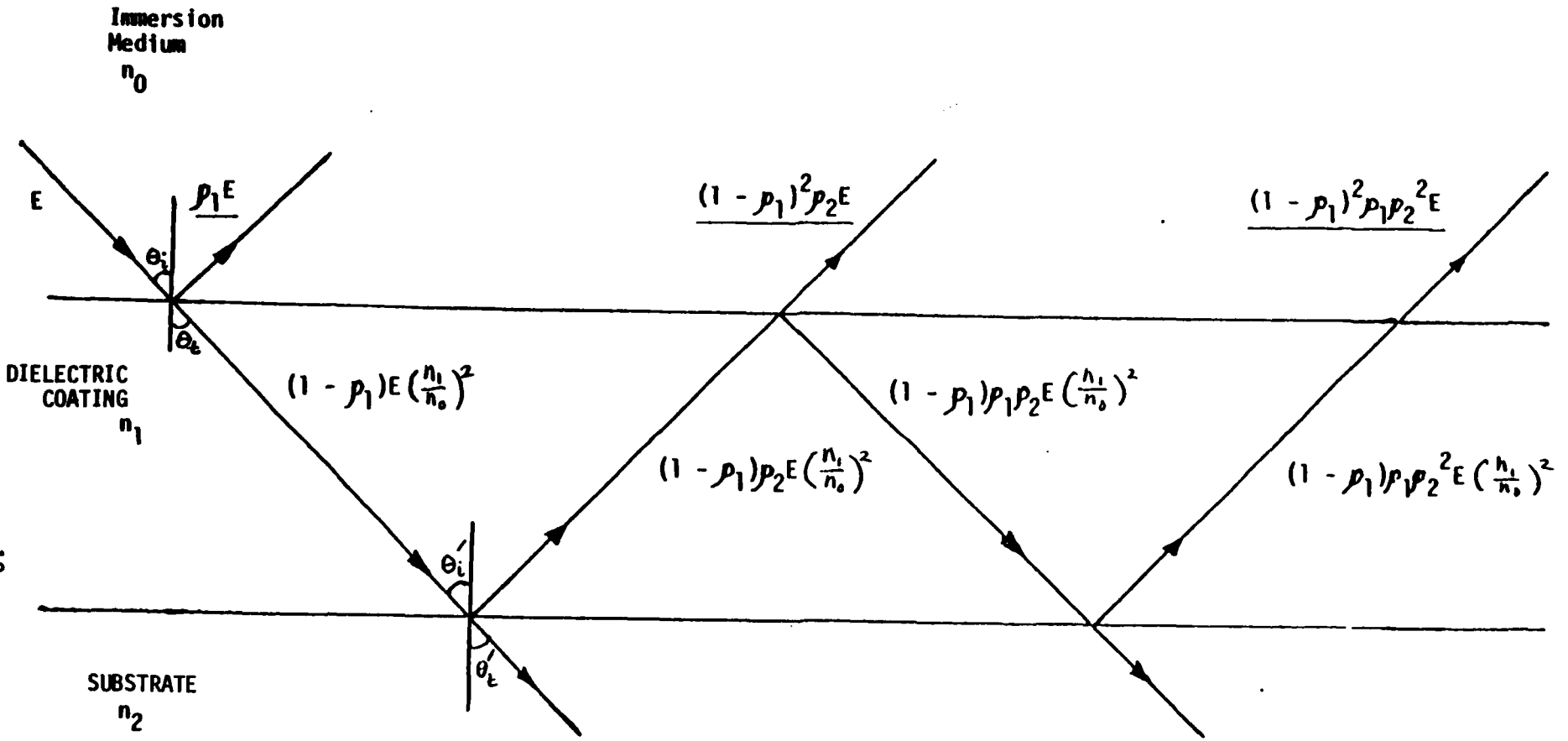

FIGURE A1. FIRST THREE TERMS OF REFLECTANCE FOR COATED MATERIAL

APPENDIX B

LIMITS TO SPIE PERFORMANCE

Summary

The spatial resolution and low-light level performance limits of SPIE are derived. The diffraction and quantum noise limits are explored and compared to anticipated off-the-shelf component performance. The off-the-shelf low light level television (L^3TV)/cystoscope system performs quite well. The eye/fiber optic/cystoscope system will perform usably if the eye is completely dark adapted, but may be useless if the eye has been recently exposed to very bright light.

PERFORMANCE SUMMARY

SYSTEM	DISTANCE TO RECOGNIZE HANDGUN	VIEWABLE SCENE
Quantum Limited L^3TV/ Diffraction Limited CYSTOSCOPE	41.7 feet	10% Reflectance illuminated by TV screen at 10 feet.
Off-The-Shelf L^3TV/ CYSTOSCOPE	14.4 feet	50% Reflectance illuminated by TV screen at 10 feet.
Dark Adapted Eye/ Fiber Optic/ CYSTOSCOPE	3.4 feet	75% Reflectance illuminated by TV screen at 10 feet.
Bright Light Adapted Eye/ Fiber Optic/ CYSTOSCOPE	0	NONE

Spatial Resolution

The fundamental limit to system resolution is the diffraction limited resolution of the cystoscope entrance pupil. Since this is a real-time system, super-resolution algorithms will not be considered.

The full angle diffraction limit will be taken to be the distance between the first zeroes of a uniformly weighted rectangular aperture impulse response:

$$\theta_R \approx \frac{2.44\lambda}{D} \quad , \tag{1}$$

where λ is the optical wavelength, and D is the diameter of the cystoscope entrance pupil.

It is assumed that the cystoscope entrance pupil diameter is 1.5 mm. From Eq. (1):

$$\theta_R \approx \frac{2.44(6 \times 10^{-7} \text{ meters})}{1.5 \times 10^{-3} \text{ meters}} \approx 1 \text{ milliradian} \quad .$$

This is about the same as the resolution of the human eye. It is not easy to construct a diffraction limited relay system consisting of 15 triplet lenses. However, if some other part of the system limits resolution to well above one milliradian, the cystoscope resolution will not be a major concern.

The resolution of off-the-shelf low light level television cameras is nominally 500 to 600 lines per picture height. It is assumed that the closed-circuit TV monitor exceeds this resolution so that the L^3TV camera is the limiting factor. If perfect coupling is achieved between the

cystoscope and the L^3TV system, the picture height corresponds to the cystoscope full angle field of view of 100°, or about 1.75 radians. An L^3TV with 600-line resolution then limits us to 2.9 milliradian resolution, or about three times the diffraction limit for the cystoscope optics. An L^3TV system with a resolution of 1800 lines per picture height would allow diffraction limited performance, if the cystoscope is capable of supporting this level of performance.

The resolution allowed by a fiber optics bundle is a function of the number of individual fibers in the bundle. A medical endoscope has typically 20,000 pixels or about $\sqrt{20,000}$ = 141 lines per picture height. This is a factor of four worse than an off-the-shelf L^3TV system, and it corresponds to a resolution of 12.3 milliradians for a 100° field of view.

It is common to take the required resolution for a 50% probability of recognition of an object in the field of view to be 3 line pairs (six TV lines) per object length. The corresponding resolution for a 95% probability of recognition is 6 line pairs (12 TV lines) per object length. Recognition is defined as the ability to classify the type of object viewed (it's a handgun, not a beer can), but not to identify it (it's a Smith & Wesson, not a Ruger). Applying the criterion that 95% probability of recognition is required in a field application, 12 lines per object length are required. This means the object must subtend an angle of 12 mr for a diffraction limited system, 34.8 mr for a 600-line L^3TV system, and 147.6 mr for a 20,000 pixel fiber bundle system. Table I illustrates the distance from the cystoscope at which each hypothesized system could resolve a 6-inch long handgun.

TABLE I

MAXIMUM DISTANCE FOR RECOGNITION OF A HANDGUN

SYSTEM	DISTANCE (FEET)
Diffraction-Limited Cystoscope	41.7
600-Line L^3TV	14.4
20,000-Pixel Fiber Bundle	3.4

Low-Light-Level Performance

The signal-to-noise ratio (SNR) available is the noise inherent in the signal itself. That is, a noiseless optical receiver will still exhibit a finite SNR at the output due to random fluctuations in the signal itself.

The variance in photon emission by an incoherent source (a source whose emission is not truly "stationary," or time-independent) is derived from Bose-Einstein statistics:

$$\sigma^2 = \bar{n}\left[\frac{e^{h\nu/kT}}{e^{h\nu/kT} - 1}\right] , \tag{2}$$

where $\bar{n}$ = the average number of photons emitted,

h = Planck's constant,

ν = the temporal light oscillation frequency,

k = Boltzmann's constant, and

T = is the absolute temperature (Kelvins).

For the very high frequencies involved in optical work ($\nu \tilde{\geq} 5 \times 10^{14}$ Hz) and ordinary temperatures ($T \tilde{\geq}$ 300 K), we have that the energy per photon is much greater than the thermal energy ($h\nu >> kT$) and:

$$\frac{e^{h\nu/kT}}{e^{h\nu/kT} - 1} \tilde{\geq} 1 . \tag{3}$$

Equation (2) reduces for our purposes to:

$$\sigma^2 = \bar{n} , \tag{4}$$

which is the result for simple Poisson statistics. Taking the signal to be the mean number of photons, and the noise to be the standard deviation in that number due to random fluctuations in emission:

$$SNR = \frac{\bar{n}}{\sigma} = \frac{\bar{n}}{\sqrt{\bar{n}}} = \sqrt{\bar{n}} \quad . \tag{5}$$

The observed SNR for a noiseless photon detector with perfect quantum efficiency can never exceed that of Eq. (5).

From the standpoint of image quality, the SNR should be 3 for detection and 6 for identification (Biberman (1973)). An SNR of 6 will be the assumed requirement for the present analysis. From Eq. (5), an SNR of 6 requires an average signal level of 36 photons per picture element per frame time for a noiseless, perfectly quantum efficient L^3TV system. If the frame time is 1/30 second and the L^3TV resolution is 500×500 pixels per frame, then the required incident photon flux is:

$$\begin{aligned} \Phi_p &= (36 \text{ phot./pixel-frame time})(500)^2 \text{pixels}(30 \text{ frames/sec}) \\ &= 2.7 \times 10^8 \text{ photons/second} \quad . \end{aligned}$$

The required photon flux density on a 30 mm diameter L^3TV tube is:

$$E_p = \frac{2.7 \times 10^8 \text{ phot./sec}}{\frac{\pi}{4}(3 \text{ cm})^2} = 3.8 \times 10^7 \text{ photons/sec-cm}^2 \quad .$$

Equation (5) of Crowe (1982) may be used, where the quantities are now understood to be in photon units, rather than lumen units:

$$E_p = \tau L_p \Omega_r \left(\frac{A_r}{A_i}\right) \quad , \tag{6}$$

where $\tau \equiv 1$ for a "lossless" system, L_p is the photon flux radiance of room objects in photons per second and steradian and square centimeter, Ω_r is the solid angle field of view of the cystoscope, A_r is the

entrance pupil area of the cystoscope, and A_i is the entrance pupil area of the L^3TV. Solving for L_p:

$$L_p = \frac{E_p}{\Omega_r\left(\frac{A_r}{A_i}\right)} = \frac{\Phi_p}{A_r\Omega_r} \tag{7}$$

We may now calculate the minimum photon flux radiance of the scene in order to provide sufficient SNR for an ideal SPIE device to identify objects in the room:

$$L_p = \frac{2.7 \times 10^8 \text{ photons/sec}}{\frac{\pi}{4}(0.15 \text{ cm})^2(2.8 \text{ steradians})} = 5.5 \times 10^9 \text{ phot./sec-cm}^2\text{-sr.}$$

This corresponds to 1.8×10^{-7} watts/cm^2 sr at $\lambda = 0.6$ micrometers. This quantity must now be converted into foot Lamberts (fL) for comparison with the results of a previous memo (Crowe (1982)).

The conversion of watts/cm^2 sr to fL requires knowledge of the spectral response of the human eye and the spectral radiance of the source:

$$\underset{\text{(foot Lamberts)}}{L_o} = k_{max} \int_0^\infty \underset{\text{(W/cm}^2\text{-sr)}}{v(\lambda)L_e(\lambda)}\,d\lambda \quad , \tag{8}$$

where $k_{max} = 673$ lumens/watt,

$v(\lambda)$ = the normalized eye spectral response, and

$L_e(\lambda)$ = the spectral radiance of the source.

Rather than attempt a numerical integration of Eq. (8) without knowing $L_e(\lambda)$ with precision, the concept of blackbody luminous efficacy will be

introduced. First we define the blackbody luminance:

$$L_o^b(T) = k_{max} \int_0^\infty v(\lambda) L_e^b(\lambda,T) d\lambda \quad , \tag{9}$$

where the superscript "b" denotes blackbody quantities:

$$L_e^b(\lambda,T) = \frac{2hc^2}{\lambda^5[e^{hc/\lambda kT} - 1]} \quad . \tag{10}$$

The luminous efficacy of a blackbody radiator is the ratio of its total luminance to its total radiance:

$$k_b(T) = \frac{\pi L_o^b(T)}{\sigma T^4} \quad , \tag{11}$$

where σ is the Stephan-Boltzmann constant $\approx 5.7 \times 10^{-8}$ W/m^{2}K^4. The absolute temperature T in Kelvins, used for specifying the sensitivity of L^{3}TV cameras, is 2854 K (a standard incandescent lamp). Figure 9 of Chapter 1 of Driscoll and Vaughn (1978) gives numerical values of $k_b(T)$. The value for T = 2854 K is approximately 17 lumens/watt. Since one foot Lambert is one lumen per square foot and steradian, we can now estimate our minimum scene luminance required for a perfect L^{3}TV/ cystoscope to recognize objects:

$$L_o \approx (1.8 \times 10^{-7} \text{ watts/cm}^2\text{-sr})(17 \text{ lumens/watt})(929 \text{ cm}^2/\text{ft}^2) = 2.8 \times 10^{-3} \text{ fL.}$$

This may be compared with the minimum scene brightness anticipated of 3×10^{-3} fL and 1.5×10^{-2} fL usable by an assumed off-the-shelf system (Crowe (1982)).

An analysis of the eye-fiber optic-cystoscope combination is complicated by the lack of unambiguous data defining the sensitivity of the eye. The data chosen here is the statement in Allen (1976) that 60 photons are required to produce a single perceptible eye scintillation. I interpret this to mean that the eye has 1/60 = 0.017 quantum efficiency. This statement presumably applies to the dark-adapted eye. The eye possesses about a 100 dB total dynamic range, and about 30 dB instantaneous dynamic range under bright conditions. I will assume the eye to be 10^{-7} times less sensitive, therefore, when bright-light adapted.

The form of Eq. (5) appropriate for quantum efficiencies (η) less than one is:

$$SNR = \sqrt{\eta\bar{n}} \quad . \tag{12}$$

The requirement that SNR = 6 with $\eta = 0.017$ implies the $\bar{n} = 2160$ photons. The cognitive integration time of the eye-brain combination is about 0.1 second, and the fiber bundle has 20,000 pixels:

$$\Phi_p = (2160)(10/\text{sec})(20{,}000) = 4.3 \times 10^8 \text{ photons/second}$$

required to recognize objects in a room. From Eq. (7):

$$L_p = \frac{\Phi_p}{A_r \Omega_r} = 8.8 \times 10^9 \text{ shot/sec-cm}^2\text{-sr}$$

which corresponds to 3.3×10^{-7} watts/cm^2-sr, at $\lambda = 0.5$ μm. Using the luminous efficacy of a 2854 K source:

$$L_o = 3.3 \times 10^7(17)(929) = 5.2 \times 10^{-3} \text{ fL} \quad .$$

The fact that this is only a factor of two worse than an L^3TV system with a quantum efficiency of one results from the longer integration time and greater spatial integration (lower resolution) of the eye. It is also unlikely that the observer can spend 40 minutes in total darkness to adapt his eye. Applying the estimated cystoscope throughput of 0.232 (Crowe (1982)):

$$L_o = \frac{5.2 \times 10^{-3}}{0.232} = 2.25 \times 10^{-2} \text{ fL} \quad ,$$

which is less sensitive than the 1.5×10^{2} fL of a projected off-the-shelf system. Degrading this performance by 10^{-7} for the fully bright-adapted eye shows that the brightest room scenes (30 fL) cannot be seen at all under some eye adaptation conditions! Table II summarizes the low light level performance.

TABLE II
LOW-LIGHT LEVEL PERFORMANCE

SYSTEM	REQUIRED SCENE BRIGHTNESS	SCENE VIEWABLE
Perfect L^3TV & Cystoscope	2.8×10^{-3} fL	10% Reflectance illuminated by TV screen at 10 feet
Off-the-Shelf L^3TV/ Cystoscope	1.5×10^{-2} fL	50% Reflectance illuminated by TV screen at 10 feet
Dark-Adapted Eye/Cystoscope	2.3×10^{-2} fL	75% Reflectance illuminated by TV screen at 10 feet
Bright Light-Adapted Eye/ Cystoscope	Up to $\sim 2 \times 10^{5}$ fL	NONE

References

L.M. Biberman, Perception of Displayed Information, Plenum Press, 1973.

D.G. Crowe, "Preliminary Performance Analysis of Low-Light Level Television/Cystoscope Combination," SAI Memo to D. Phillips, et al., July 20, 1982

W.G. Driscoll and W. Vaughn, (eds.), Handbook of Optics, McGraw-Hill, 1978.

C.W. Allen, Astrophysical Quantities, Athlone Press, University of London, 1976.

APPENDIX C

SILENT DRILLING

1.0 INTRODUCTION

It is possible to make drills which are very quiet when they are running, but they are not in contact with the surface to be drilled. Very loud sound is generally produced when the rotating drill is in contact with, for example, a wall. Peter Franken has suggested a possible method to cancel this sound.

The proposed method is to sense the wall displacement which produces the sound, and to drive the wall in such a way that the displacement is reduced nearly to zero. The brief analysis which follows serves to document that:

1. The method will certainly work in theory for some ideal cases, and
2. The real world case is sufficiently complex that experiments should be carried out to determine the usefulness of the method.

2.0 THE ONE-DIMENSIONAL PROBLEM

2.1. Single Frequency

The mechanical displacement as a function of time for a single frequency driven by the drill is:

$$U(t) = A_0 \cos(\frac{2\pi t}{\tau} - \phi_0), \tag{1}$$

where A_0 is the amplitude, τ is the period, and ϕ_0 is the phase. If we introduce a second excitation into the wall at the same frequency:

$$U(t) = A_0 \cos(\frac{2\pi t}{\tau} - \phi_0) + A_1 \cos(\frac{2\pi t}{\tau} - \phi_1). \tag{2}$$

If the phases differ by half a period:

$$U(t) = (A_0 - A_1)\cos(\frac{2\pi t}{\tau} - \phi_0). \tag{3}$$

Inspection of (3) implies the well-known result that if $A_0 = A_1$, then $U(t) \equiv 0$; that is, an out-of-phase excitation of equal amplitude can cancel the sound level to zero.

For this simple case, it is easy to see how the original signal of equation (1) may be used to drive an electro-mechanical network to produce the excitation required to cancel the sound level. In Figure 1, the drill is modelled as a linear motor which drives the wall with the displacement of equation (1). A pickup transducer (e.g. phonograph cartridge or microphone) is placed within a small fraction of a wavelength so that it generates an electrical signal essentially in phase with the wall displacement and proportional to its amplitude:

$$E_1(t) = \frac{A_0}{K_1} \cos(\frac{2\pi t}{\tau} - \phi_0), \tag{4}$$

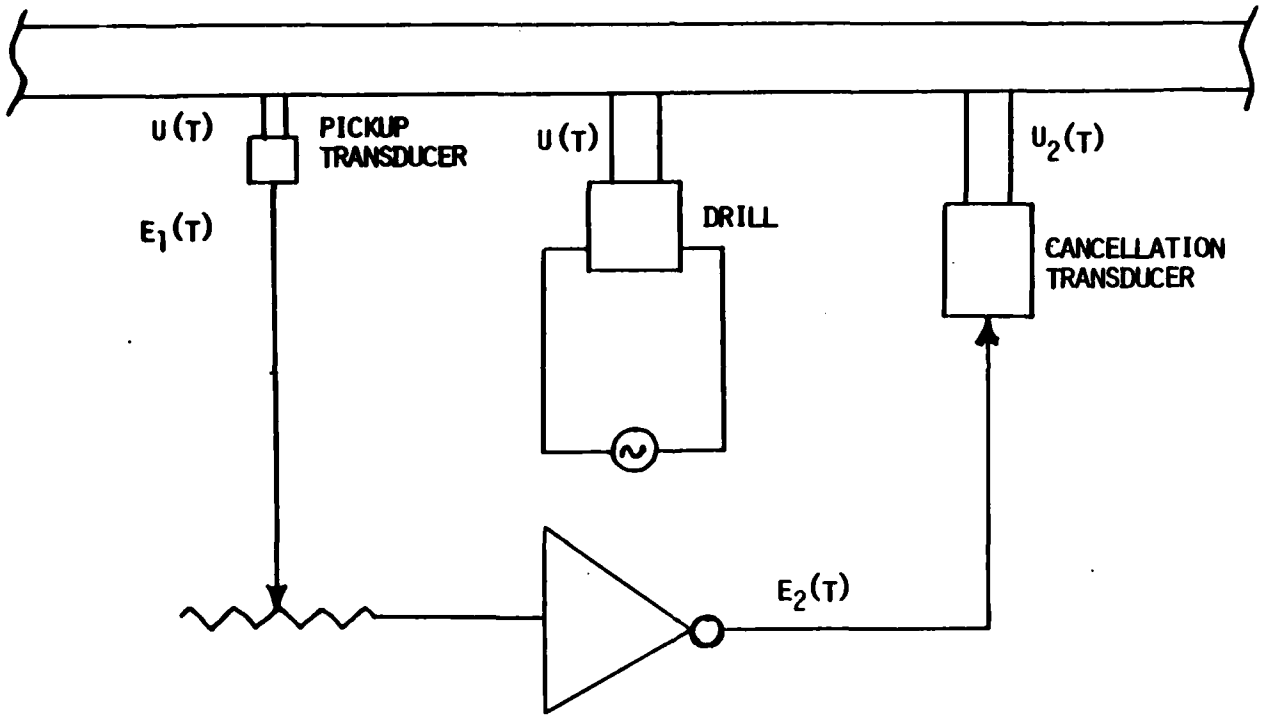

Figure 1. Sound Cancelling Electro-Mechanical Network

Assume that the output transducer (e.g. loudspeaker) produces a wall displacement proportional to the electrical signal presented to it:

$$U_2(t) = \frac{E_2(t)}{K_2} \tag{5}$$

Then by adjusting the gain of the phase inverting amplifier to K_1K_2:

$$U_2(t) = [\frac{A_o}{K_1}\cos(\frac{2\pi t}{\tau} - \phi_o)](-K_1K_2)(\frac{1}{K_2})$$

$$= -A_o \cos(\frac{2\pi t}{\tau} - \phi_o), \tag{6}$$

which is just the displacement required for zero resultant sound output from the wall. Additional circuitry would be added in practice to actively adjust the gain for minimum displacement of the input transducer. It has been assumed that the distance between the three transducers of Figure 1 is very small compared to a wavelength. The speed of sound in a solid wall is on the order of several thousand feet per second. Therefore, if the drill excites the wall at 200 Hz, the wavelength is about 10 or 20 feet, and the near-field assumption is easy to achieve in practice.

2.2. Multiple Frequencies

If the wall is excited by a complex driving function composed of multiple frequencies, the displacement becomes:

$$U(t) = \sum_{i=1}^{n} A_i \cos(\frac{2\pi t}{\tau_i} - \phi_i). \tag{7}$$

The network of Figure 1 still cancels the sound, however:

$$U_2(t) = [\frac{1}{K_1}\Sigma A_i \cos(\frac{2\pi t}{\tau_i} - \phi_i)](-K_1K_2)(\frac{1}{K_2}) \tag{8}$$

$$= \Sigma - A_1 \cos(\frac{2\pi t}{\tau_i} - \phi_i).$$

This may be viewed as driving the wall with the negative of the resultant displacement:

$$U_2(t) = -U(t). \tag{9}$$

This way of describing the problem eliminates the complication of worrying about how to eliminate each spectral component individually. The operation of equation (9) can be realized in practice for linear (distortion-free) input and output transducers and investing amplifier if and only if this electro-mechanical network has a uniform frequency response over the required range. Input low-pass filtering is recommended to prevent system response outside the frequency range for which the near field assumption is valid.

3.0. THE TWO-DIMENSIONAL PROBLEM

Consider a membrane of infinitesimal thickness under tension T. A small area S on the membrane experiences a restoring force perpendicular to the membrane of:

$$T \oint \frac{\partial w}{\partial n} ds,$$

where w is the displacement perpendicular to the rest plane of the membrane, ∂n is an element normal to the boundary element ds and the integral is performed around the boundary of S. From Green's theorem:

$$\oint \frac{\partial w}{\partial n} ds = \iint_S \nabla^2 w \, dS. \tag{10}$$

Therefore the equation of motion is:

$$\frac{\partial^2 w}{\partial t^2} = \frac{T}{\rho} \nabla^2 w = v^2 \left(\frac{\partial^2 w}{\partial x^2} + \frac{\partial^2 w}{\partial y^2} \right), \tag{11}$$

where ρ is the density of the membrane and v is the speed of sound in the membrane. By choosing a particular shape for the boundary of S and imposing the boundary condition w=0, the nature of the vibrational modes of the membrane may be deduced from equation (11).

For a rectangular boundary bounded by the lines x=0, y=0, x=a, y=b, the general solution is [1]:

$$w = \sum_{m=1}^{\infty} \sum_{n=1}^{\infty} \sin\left(\frac{m\pi x}{a}\right)\sin\left(\frac{n\pi y}{b}\right)[A_{mn}\cos pt + B_{mn}\sin pt]. \qquad (12)$$

where:

$$p = \pi v\left(\frac{m^2}{a^2} + \frac{n^2}{b^2}\right)^{1/2}. \qquad (13)$$

The nodes are lines parallel to the x and y axes defined by the equations:

$$x = \frac{a}{m}, \frac{2a}{m}, \ldots \frac{(m-1)a}{m},$$
$$y = \frac{b}{n}, \frac{2b}{n}, \ldots \frac{(n-1)b}{n}. \qquad (14)$$

The modes for rectangular membranes are therefore rectangular areas of vibrational displacement with the displacement maximum at the center of the rectangles and zero at the edges. For circular boundaries, the modal patterns are combinations of straight lines through the center (diameters) and circles concentric with, but of less diameter than, the boundary (Figure 2, after [1]).

A wall is, in reality, not a membrane but a plate of possibly variable thickness and sound velocity. The modes are therefore not in general predictable. The form of equations (14) suggests, however, that a complex pattern of vibrations and nodes will form such that a single sound cancelling transducer can work successfully only if it is close to the drivers compared to the shortest wavelength of sound produced. Equation (12) indicates that there is no shortest wavelength for an ideal membrane. The shortest wavelength of interest is set by the upper limit to the human ear response, about 20kHz. This corresponds to a wavelength of order 1 centimeter in a solid. It is likely, therefore, that complete cancellation of all components is not possible. It is also likely, however, that for a low driving frequency (e.g. 200 Hz), the high frequency components will not be large in amplitude.

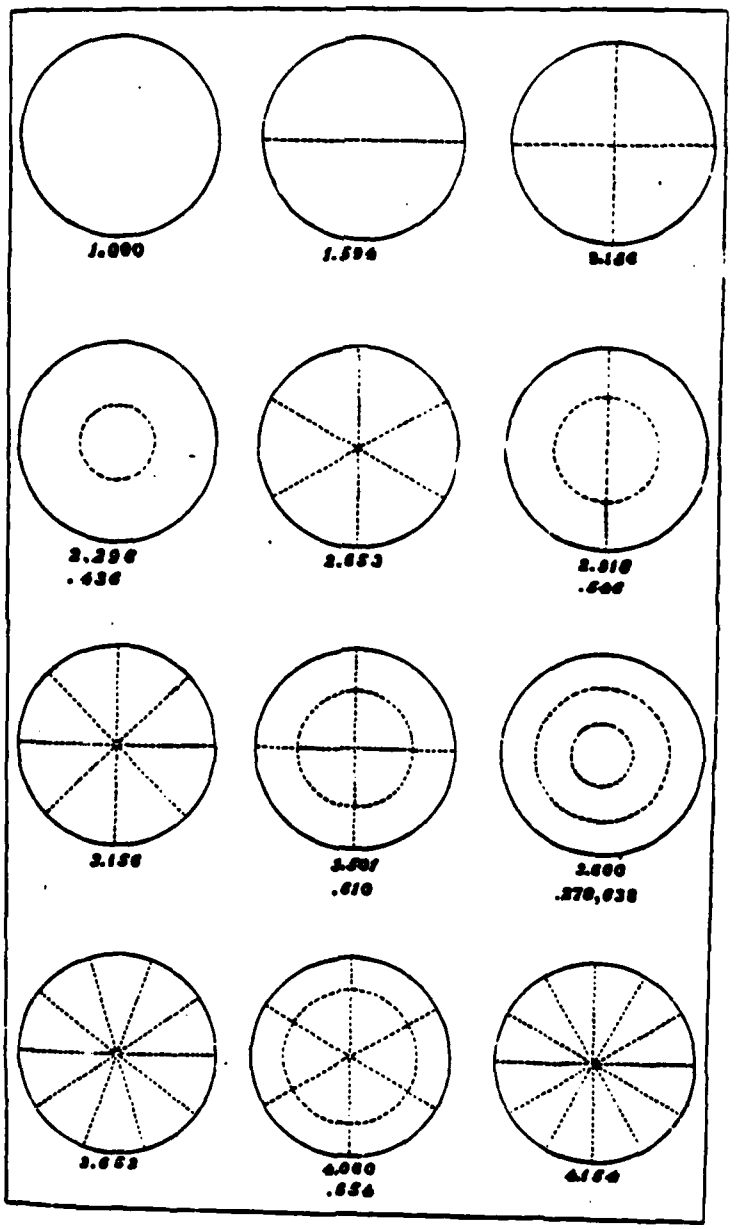

Figure 2. Nodes of a Circular Membrane [After Rayleigh (1877)].

4.0 ISSUES

The cancellation of sound is a complex problem. The brief theoretical introduction presented here suggests that a useful reduction in sound level may be achieved by simple means. A number of possible sources of difficulty can be identified, but their importance is difficult to estimate in the absence of experimental data. Some of these are listed below:

- Will high frequency sound be generated by flexing of the wall between the drill and the sound cancellation transducer?
- Will a simple scheme such as that illustrated in Figure 1 cancel frequencies (intermodulation products) which arise as the result of nonlinear wall response to displacement drivers?
- Can a complex wall construction cause asymmetrical node patterns such that a node appears close to the driver compared to a wavelength? This could negate the usefulness of the proposed scheme in some cases. (Consider the complex boundary value problem presented by drilling near wall studs.)
- Since monopole, dipole, quadrapole, and higher order radiation patterns may be present, is it possible that the pickup transducer could be in the near field yet in a null direction and thus fail to detect significant sound components?

REFERENCE

1. Rayleigh, J.W.S., The Theory of Sound, Dover (1945), [First published 1877, revised 1894).

APPENDIX D

SOUND CANCELLATION SENSITIVITY ANALYSIS

1.0 INTRODUCTION

The amount of sound cancellation attainable by using a second, out-of-phase source is a function of source size, source separation, and observer direction. A brief discussion of these functional dependencies shows that the cancellation is quite sensitive to source size and separation. For many practical configurations, the amount of cancellation which is possible is rather small, particularly at the higher frequencies.

2.0 DISCUSSION

Consider a single frequency source which we will attempt to cancel:

$$V(t) = A_0\cos(\frac{2\pi t}{\tau} - \phi_0). \qquad (1)$$

For the moment assume that this is a point source, and that we will place a second point source a distance S from the first. Then, in the far field, an observer will detect a sound intensity as a function of separation (S), phase (ϕ_1), and direction (θ in Figure 1):

$$I(t) = \{A_0\cos(\frac{2\pi t}{\tau} - \phi_0) + A_1\cos[\frac{2\pi t}{\tau} - (\phi_1 + \frac{S\cos\theta}{\lambda})]\}^2, \qquad (2)$$

where the wavelength is the period multiplied by the speed of sound ($\lambda = v\tau$). The resultant intensity of the two sources may be compared to the intensity of the first source alone on a deciBel scale:

$$dB = 20\text{Log}_{10}\left\{\frac{A_0\cos(\frac{2\pi t}{\tau} - \phi_0) + A_1\cos[\frac{2\pi t}{\tau} - (\phi_1 + \frac{S\cos\theta}{\lambda})]}{A_0\cos(\frac{2\pi t}{\tau} - \phi_0)}\right\} \qquad (3)$$

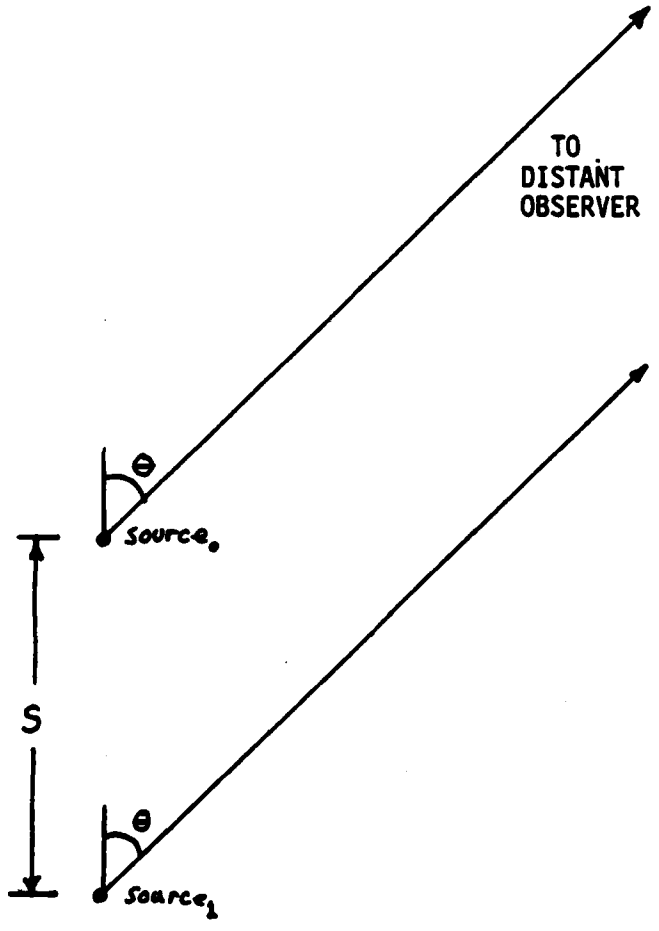

FIGURE 1. NOISE ($source_0$) AND CANCELLATION ($source_1$) GEOMETRY

As an example, choose $\theta = 0$, $\phi_0 = 0$, $\phi_1 = \pi$, $A_0 = A_1$. This will demonstrate the separation sensitivity of an out-of-phase cancellation source (Table 1).

Table 1. Separation Sensitivity of Sound Cancellation

Relative Intensity (dB)	Separation (λ)
+6	$\lambda/2$
+4.6	$3\lambda/2$
0	$\lambda/4$
-6	$\lambda/6$
-10.6	$\lambda/8$
-22	$\lambda/16$
-34	$\lambda/32$
-46	$\lambda/64$
$-\infty$	0

The separation column of Table 1 can also be viewed as the relative phase error for zero separation. For example, if the separation is zero, but the relative phase is $\pi - \frac{2\pi}{8}$, the relative intensity is -10.6 dB. Note that a gross separation or phase error can result in a sound enhancement of up to +6 dB. At the other limit (small separation or phase error), it will be noted that halving the separation or phase error will reduce the intensity 12 dB.

The ear has a non-linear response such that 3 dB is barely noticed, and 10 dB is not a large difference. Yet 10 dB of sound reduction required $\lambda/8$ separation in Table 1, or just 2-1/2 inches in air at 500 Hertz. To reach -46 dB, a tiny separation of 3/8" is required at 500 Hertz (alternately, an electrical phase error of only 5.6°). This tiny separation is probably not achievable with real components. The fact that sound cancellation in solids is aided by increased wavelengths is only a partial solution. Very large cancellations with real components will only be feasible for very low frequencies.

If we now assume that the sources have finite but equal diameters d, and that the distributions of sound intensities over the finite surfaces are random and independent, the effective separation is on the order of:

$$S_{eff} = \sqrt{d^2 + s^2} \qquad (4)$$

Thus, without prior knowledge of the complex intensity distributions over the source, we cannot assume that the effective separation is less than the source diameter. This raises the serious question (which can only be settled experimentally) of whether a large wall must be treated as the source or only as the propagation medium. A more deterministic example is a common 6 inch loudspeaker in air. The sound produced by this radiator probably can not be reduced in all directions by more than 22 dB at 100 Hertz, 10.6 dB at 200 Hertz, or 6 dB at 400 Hertz. That is, at least one direction can be found for the examples above in which the sound intensity is attenuated by the indicated factor, or less.

APPENDIX E

UHF T.V. JAMMING

1.0 RELATIVE SUSCEPTIBILITY

Home television receivers (UHF or VHF) are not designed to be tolerant of potential active interference sources for economic reasons. As a mass-market consumer electronic product, TV receivers are not subjected to significant active interference in a large fraction of home installations.

An index of relative susceptibility will be used to illustrate that T.V. receivers are exceptionally susceptible. The index is defined as:

$$\chi_r \equiv 10 \text{ LOG}[\frac{G \Delta f K}{F k T}] \quad , \tag{1}$$

where χ_r is the relative susceptibility in dB, G is the antenna gain (or loss), Δf is the bandwidth, K is a Joule-second to generate a unitless ratio, F is the noise factor, k is 1.4×10^{-23} J/K, and T is the temperature in Kelvins. This definition is a statement that the wider the bandwidth and the more sensitive an electronic device, the more susceptible it is. Many factors have been ignored, but this simple index seems adequate to compare the susceptibility of electronic devices not designed with ECCM in mind (Table 1). Note that a T.V. receiver is more susceptible than other home entertainment devices.

Table 1. Relative Susceptibility of Electronic Devices

DEVICE	RELATIVE SUSCEPTIBILITY (χ_r)
Audio Amplifier	∿100 dB*
AM Radio	∿200 dB**
FM Radio	240 dB
T.V. Receiver	260 dB

* Estimated - depends on shielding

** Estimated - sensitivity limited by external noise

2.0. JAMMER HARDWARE

A quick look through the Microwaves Product Data Directory 1980/1981 produced the following off-the-shelf hardware combinations. It should be noted that Raytheon has a "design to cost" ECM program, but the "cost" is generally high, as is the unit volume.

2.1. Jamming the Entire Band.

In the U.S., the UHF T.V. channels are contained between 470 and 806 MHz. Each channel is 6 MHz wide. Jamming all possible channels requires broadband equipment with sufficient power to insure that each 6 MHz channel is jammed.

The brute force method to accomplish broadband jamming is to broadcast "white" noise across the entire spectrum of interest. The required carrier to noise ratio (C/N) to insure that no information is received will be estimated by the use of ad-hoc model for the fraction of the total pixels per picture which are lost:

$$\varepsilon(C/N) = 1 - \frac{2}{\sqrt{\pi}} \int_0^{C/N} e^{-t^2} dt = \frac{2}{\sqrt{\pi}} \int_{C/N}^{\infty} e^{-t^2} dt. \qquad (2)$$

It will be assumed that 0.9 of the pixels must be lost, since the eye and brain might be able to integrate a useable picture with 0.5 of the pixels. The required C/N from (2) is about 0.08, that is, the noise must be about 12 times as strong as the signal to guarantee jamming. Assuming that a 100 Kw ERP transmitter is located one mile from the T.V. receiver, the jammer must produce an ERP of 120 watts if it is located 50 feet from the receiver and 0.12 watts if it is only 1.5 feet from the receiver antenna. The required power outputs of the jammer final amplifier are 10 watts and 0.01 watts respectively if an antenna gain of 12 is available. These power levels are for a single 6 MHz band. Covering, say, 600 MHz to insure coverage of all UHF channels (including those in foreign countries which may lie outside the U.S. 336 MHz segment) requires a total power of 1000 watts for a remote jammer and 1 watt for a proximity jammer.

Figure 1 depicts two broadband white noise proximity jammers. Figure 1A uses a 15 dB noise source which produces a signal of 10^{-10} watts in 600 MHz at 300K. The amplifiers can produce 108 dB of total gain and a maximum output of 2 watts. The all solid state jammer would be quite light weight and compact so that it could be placed near a roof-mounted antenna or on the other side of a wall from a T.V. set mounted antenna and left unattended with battery power. The components identified in Figure 1A cost about $6,000. Figure 1B depicts five inexpensive amplifiers in cascade with the first amplifier serving as the noise source. The four following amplifiers are capable of 108 dB total gain and a maximum output power of 1 watt. This is still a fairly compact solid-state system which costs $2,250.

A brute force remote jammer can be fabricated using one of the proximity jammers of Figure 1 to drive a high power broadband amplifier. Amplifier Research makes special Series H amplifiers to 1,000 watts output on a custom basis. This power level at UHF frequencies represents a serious health hazard.

An alternative approach to broadband noise is to use a sweep oscillator to drive a power amplifier. Figure 2 illustrates this configuration. The Wavetek 1004 costs $1,625 and can sweep 500 to 1,000 MHz. The model 2002A can sweep any portion of 1 MHz to 2,500 MHz and can also be used as a stable C.W. source for single channel jamming at a cost of $3,800. The Mini-Circuits ZHL-2-8 is a one watt broadband amplifier covering 1 MHz to 1,000 Mhz for $450.00. The swept frequency configuration offers lower cost, complexity, and weight with the advantage of placing pulses of full peak power into each channel during each sweep. This configuration is recommended.

2.2. Single Channel Jamming.

A tuneable C.W. source and amplifier such as the Wavetek 2002A and Mini-Circuits ZHL-2-8 of Figure 2 can be used to jam a single channel. The same equipment can also sweep in frequency and be used for both single channel and broadband jamming.

For remote jamming at extreme distances, the Epsco Microwave PG5KB High Power Pulsed Signal Source with the Model 5233H/B3 Oscillator Plug-In can be tuned to a single frequency from 450 to 950 MHz. The pulse width is 0.3μsec so that the bandwidth of about 3 MHz is well suited to this application. The high peak power of 5,000 watts concentrated in a single channel means that the signal from a 100 Kw T.V. transmitter only one mile from the source can be jammed from a distance of 1,000 feet.

The determination of the frequency of a UHF channel in a foreign country could present a problem. The most elegant solution available is a portable ELINT receiver. For example, Andersen Laboratories can supply receivers which search a 500 MHz bandwidth in 0.5μsec for a resolution of 3 MHz and 100% probability of intercept.

3.0. CONCLUSIONS

A proximity swept frequency jammer which jams the entire UHF band can be constructed from components costing a little over $2,000. This lightweight, solid-state device could be left in the proximity of the T.V. antenna operating with battery power.

A combination stable C.W./swept frequency jammer can be constructed to offer a choice of operating mode.

High power pulsed signal sources are available to allow jamming from sites hundreds of meters away from the T.V. set. The power levels involved are health hazards because human body tissues absorb at UHF frequencies and heating results which can cause serious burns and possibly death.

An ELINT receiver can determine the frequencies of all local UHF transmitters if selective jamming is contemplated.

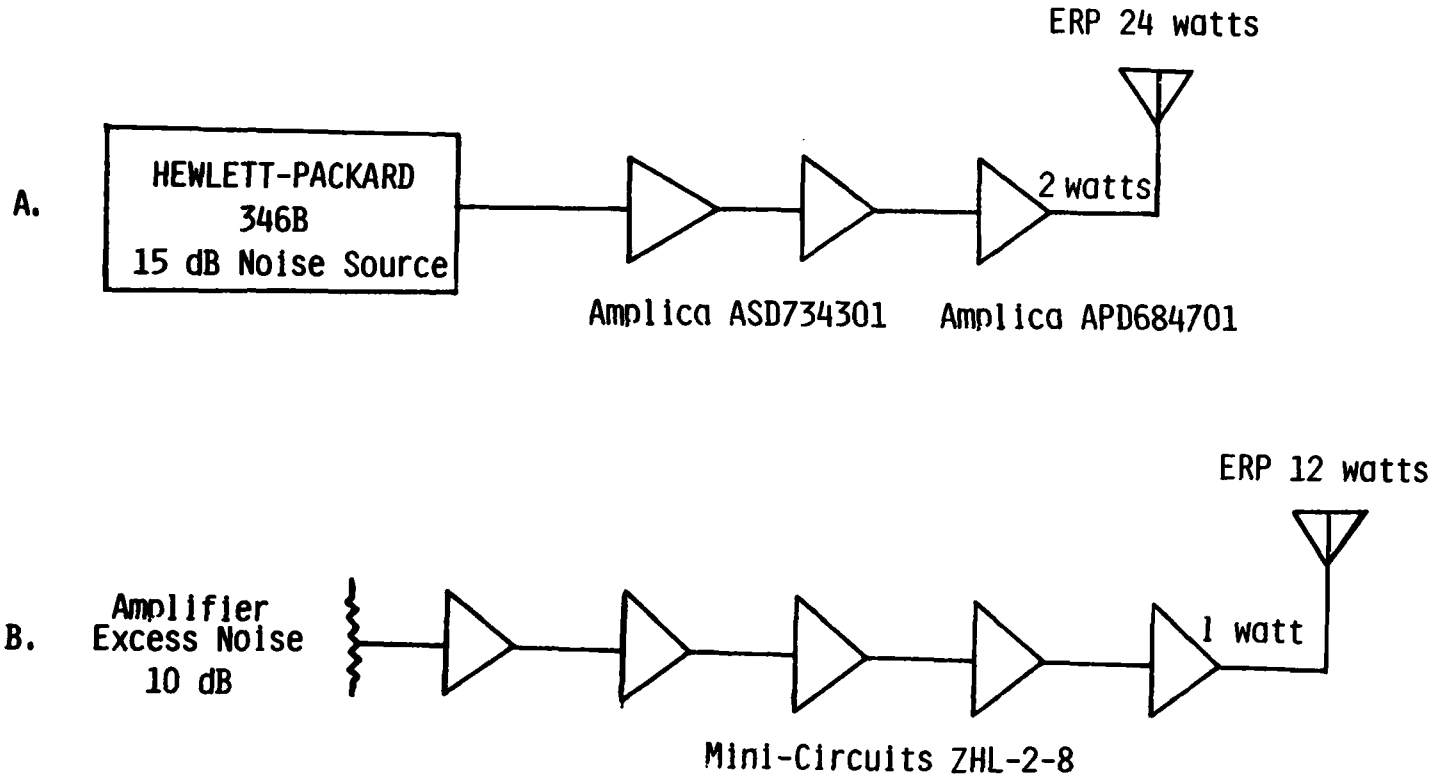

Figure 1. Brute Force Proximity Jammers

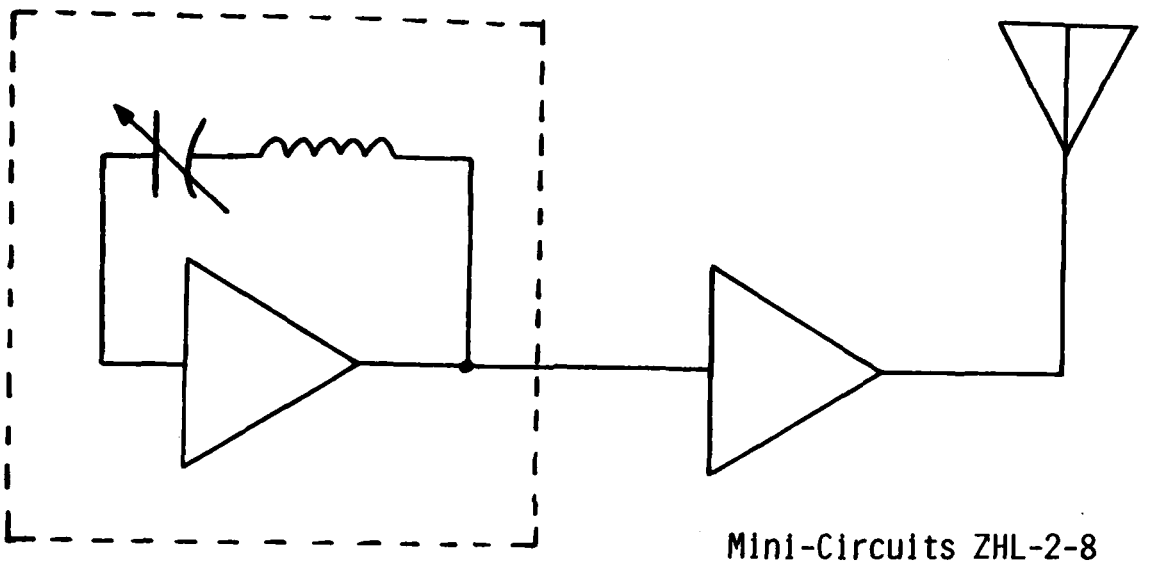

Figure 2. Swept Frequency Jammer

END

DATE
FILMED

10 83

DTIC